18,12

Thermophoresis of carbon nanoparticles (nanoribbons and nanotubes) on a flat multilayer substrate of hexagonal boron nitride (h-BN)

© A.V. Savin

[1] N.N. Semenov Federal Research Center of Chemical Physics, Russian Academy of Sciences, Moscow, Russia
[2] Plekhanov Russian University of Economic, Moscow, Russia

E-mail: asavin@center.chph.ras.ru

Received July 28, 2021
Revised July 28, 2021
Accepted August 8, 2021

Using the method of molecular dynamics and a 2D chain model, it is shown that thermophoresis of carbon nanoparticles (nanoribbons and nanotubes) on a flat multilayer substrate (on a flat surface of a hexagonal boron nitride crystal) has high efficiency. Placing a nanoparticle on a flat surface of a substrate involved in heat transfer leads to its movement in the direction of the heat flow. The heat flow along the substrate leads to the formation of constant forces acting on the nanoparticle nodes (thermophoresis forces). The main effect of the force is exerted on the edges of graphene nanoribbons, exactly where the main interaction of the nanoribbon with the bending phonons of the substrate occurs. These phonons have a long free path, so the effective transfer of nanoparticles using thermophoresis can occur at sufficiently large distances. The motion of carbon nanoparticles under the action of a heat flow has the form of particle motion in a viscous medium under the action of a constant force. Over time, the nanoparticles always enter the mode of movement at a constant speed. The velocity of the stationary motion is almost the same for all sizes and types of carbon nanoparticles, which is explained by the fact that the thermophoresis force and effective friction have the same source — the interaction of the nanoparticle with the bending thermal vibrations of the substrate layers.

Keywords: nanoribbons, nanotubes, flat multilayer substrates, thermophoresis, 2D model of the multilayer substrate.

DOI: 10.21883/PSS.2022.14.54352.178

1. Introduction

Thermophoresis is a directed particles motion, caused by a presence of external thermal gradient. Most recently the thermophoresis became a new method of nanoscale particles manipulation [1–3]. Two-dimensional (2D) lamellar materials, such as graphene (G), hexagonal boron nitride (h-BN), molybdenum disulfide (MoS_2) and tungsten disulfide (WS_2), with good thermal conductivity and low surface friction, can be used as a platform for nanoscale bodies transportation [4].

Modeling of the directed motion of nanoparticles on a flat surface of graphene sheet was performed in many works. For instance, the modeling of a cluster motion of aurum atoms Au_{459} showed, that on a flat graphite surface the cluster can demonstrate a „ballistic“ high-speed dynamics mode with viscous friction [5]. Modeling of the cluster motion over graphene sheet under a heat flow action [6] showed, that the cluster has the ballistic mode of directed motion, that is caused by the cluster interaction with bending phonons of the sheet. Analysis of motion of fullerene molecule C_{60} and short carbon nanotubes on the graphene sheet [7,8] showed the presence of two thermophoresis modes: diffusion (at low temperatures) and ballistic (at high temperatures). Modeling of graphene nanoplatelets transfer over the graphene sheet is performed in [9]. It is showed, that temperature gradient plays a critical role in nanoplatelet motion evolution. Simulation of dynamics of water nanodrop $(H_2O)_{1200}$ over the surface of the graphene sheet and hexagonal boron nitride (h-BN) showed [10], that the drop interaction with the heat flow results in its directional motion. The drop interacts stronger with surface of h-BN sheet and moves faster over it. In the work [11] it is shown, that fast dynamics of particles on a flat surface can be related to the fact, that the particle can move over graphene layer synchronously with the running bending surface wave, constantly remaining in this wave pit.

Thermophoresis phenomenon was also actively modelled for nanoparticles located inside carbon nanotubes: for individual atoms [12], atom clusters [13,14], nanodrops of water [15–20], embedded nanotubes [21–23] and molecules of fullerene C_{60} [24,25]. Interaction of these nanoparticles with thermal backgrounds flow always results in their directed motion from a warm nanotube end to a cold one.

The purpose of this work is a numerical modeling of carbon nanoparticles (nanoribbons and nanotubes) thermophoresis on the flat multilayer substrate of hexagonal boron nitride (h-BN) — see Fig. 1. It will be demonstrated, that nanoparticle placing on the flat multilayer substrate, participating in heat transfer, results in its motion with

constant speed v_s towards heat transfer. This speed value is almost the same for all sizes and types of carbon nanoparticles. Dynamics have a form of ballistic motion of particles in viscous medium under constant force action. Here the thermophoresis force and effective friction have the same source —nanoparticle interaction with the bending thermal vibrations of the substrate layers.

The work is structured as follows. Section 2 contains information on creation of 2D chain model, used further for modeling of carbon nanoparticles (nanoribbons and nanotubes) motion over the flat multilayer substrate of h-BN. Section 3 contains information on modeling of nanoparticles free motion deceleration as a result of their interaction with thermalized substrate. Section 4 contains information on determination of thermophoresis forces distribution along the nanoparticle, caused by the nanoparticle atoms interaction with the heat flow, going along the substrate. Section 5 contains information on modeling of nanoparticles flow-induced motion. Conclusion is presented in section 6.

2. Model

2D-model of the molecular chains system [26–28] can be conveniently used for description of dynamics of the carbon nanoparticles (nanoribbons and nanotubes) on the flat surface of multilayer substrate. Let's examine the flat surface of h-BN crystal as a substrate. Let's assume, that the nanoparticle and sheets of h-BN substrate are laid in such a way, that their zigzag direction coincides with x axis — see Fig. 1. In this case the two-dimensional chain model will describe a cross section of a system *nanoparticle + multilayer substrate* along x axis. One node in the model will correspond to all nanoparticle (substrate layer) atoms with the same coordinates x, z.

If atoms, located along single line parallel to y axis, moves synchronously, changing only coordinates x, z, the Hamiltonian of a single nanoribbon (nanotube) of graphene (h-BN) will have a Hamiltonian form of a chain, located in xz plane:

$$H_i = \sum_{n=1}^{N} \frac{1}{2} M_i(\dot{\mathbf{u}}_n, \dot{\mathbf{u}}_n) + \sum_{n=1}^{N-1} V_i(R_n) + \sum_{n=2}^{N-1} U_i(\theta_n), \quad (1)$$

where index $i = 1$, if we examine a nanoribbon of graphene (G), and $i = 2$, if we examine a nanoribbon of boron nitride (BN). Two-dimensional factor $\mathbf{u}_n = (x_n, z_n)$ sets the coordinates of n-th particle of the chain. Particle mass for G chain coincides with carbon atom mass $M_1 = M_C = 12m_p$, and for BN chain — with average mass of boron and nitride atoms $M_2 = (M_B + M_N)/2 = 12.4085m_p$ ($m_p = 1.6603 \cdot 10^{-27}$ kg — proton mass).

The potential

$$V_i(R) = \frac{1}{2} K_i (R - R_i)^2, \quad (2)$$

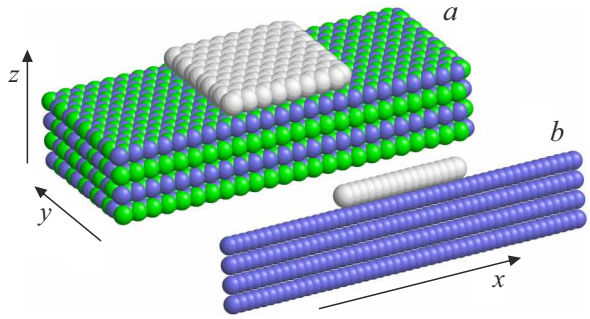

Figure 1. Creation of 2D chain model of graphene nanoribbon, laying on the flat surface of h-BN crystal. Rectangular graphene sheet (a) is shown with size of $2.02 \times 1.88\,\text{nm}^2$ (160 carbon atoms), laying on the flat multilayer h-BN substrate, as well as the corresponding two-dimensional chain model of the system (b).

describes the longitudinal stiffness of the chain, K_i — the stiffness of the interaction, R_i — the equilibrium „valence" bond length (chain pitch), $R_n = |\mathbf{u}_{n+1} - \mathbf{u}_n|$ — distance between neighboring nodes n and $n + 1$.

The potential

$$U_i(\theta) = \epsilon_i \left[1 + \cos(\theta)\right], \quad (3)$$

describes the bending stiffness of the chain, θ — the angle between two adjacent „valence" bonds,

$$\cos(\theta_n) = -(\mathbf{v}_{n-1}, \mathbf{v}_n)/R_{n-1}R_n, \text{ vector } \mathbf{v}_n = \mathbf{u}_{n+1} - \mathbf{u}_n.$$

Parameters of potentials (2), (3) for the G chain are defined in [26,27] from analysis of dispersion curves of graphene nanoribbon. Longitudinal stiffness $K_1 = 405$ N/m, chain pitch $R_1 = r_{CC}\sqrt{3}/2 = 1.228$ Å ($r_{CC} = 1.418$ Å — length of valence bond C−C in graphene sheet), energy $\epsilon_1 = 3.5$ eV.

Nanoribbon of h-BN has the same structure as graphene nanoribbon. In two-dimensional model its Hamiltonian will also have the form (1). Nanoribbon of h-BN was examined for obtaining the parameters of BN chain. Nanoribbon atoms interaction was described with extended Tersoff potential for boron nitride [29]. The calculations showed, that nanoribbon of h-BN has the same hexagonal structure as graphene nanoribbon. Length of the valence bond of B−N $r_{BN} = 1.445685$ Å in the ground state insignificantly exceeds the length of the valence bond of C−C. Dispersion curves of two-dimensional chain with Hamiltonian (1) correspond the best to dispersion curves of all-atom model of nanoribbon at stiffness $K_2 = 480$ N/m, chain pitch $R_2 = r_{BN}\sqrt{3}/2 = 1.252$ Å and energy $\epsilon_2 = 1.10$ eV.

Hamiltonian of the chain (1) gives the nanoribbon energy, falling on the longitudinal band of a width $\Delta y = R_i/\sqrt{3}$. Therefore, if the chains system energy will be further normalized by graphene nanoribbon, the energy of nanoribbons of h-BN should be multiplied to the normalizing factor $c = R_1/R_2 = 0.9808$.

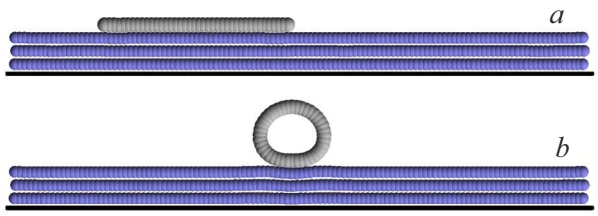

Figure 2. Form of stationary state (a) of a single-layer graphene sheet with a length $L = 4.79$ nm (number of links of a G chain $N_c = 40$) and (b) single-layer nanotube with chirality index (20,0) (number of links of a cyclical chain $N_c = 40$) on a multilayer substrate, formed by a surface of h-BN crystal (number of substrate layers $K - 1 = 3$, number of links in BN chain $N_{bn} = 360$. The black line indicates the position of stationary substrate surface.

Lennard–Jones potentials (6,12) were used for calculation of an effective potential of non-valence interaction of the chain nodes (energy of single atom interaction with transverse atoms line)

$$V(r) = \epsilon_0\left[(r_0/r)^{12} - 2(r_0/r)^6\right], \tag{4}$$

with values of energy ϵ_0 and equilibrium interaction lengths r_0, presented in Table 1.

The performed calculations showed, that interactions of the chain nodes, corresponding to layers of boron nitride substrate and graphene layer, can be described with high accuracy using the Lennard–Jones potential (5, 11)

$$W_i(r) = \varepsilon_i\left[5(r_i/r)^{11} - 11(r_i/r)^5\right]/6, \tag{5}$$

where r — distance between the interacting nodes (index $i = 1$, if interaction of the chain nodes of BN is described, $i = 2$ — interaction of the chain nodes of BN and G). Interaction energy $\varepsilon_1 = 0.01511$, $\varepsilon_2 = 0.01433$ eV, equilibrium distances $r_1 = 3.642$, $r_2 = 3.701$ Å.

Number of layers should be limited when modeling the dynamics of a multilayer substrate. Therefore, let's assume, that the first (bottom) layer already interacts with stationary flat surface of a crystal (in Fig. 2 this surface is shown with a black line).

Calculations show, that potential of interaction with stationary substrate of $W_0(h)$ (dependence of the chain node energy on distance h to substrate plane) can be described with high accuracy using (k, l) Lennard–Jones potential

$$W_0(h) = \varepsilon_0\left[k(h_0/h)^l - l(h_0/h)^k\right]/(l-k), \tag{6}$$

where degree $l = 10$, $k = 3.75$, interaction energy $\varepsilon_0 = 0.0974$ eV, equilibrium distance $h_0 = 3.49$ Å.

Let's examine K-layer structures, presented in Fig. 2. Let's assume, that the first $k = 1, \ldots, K-1$ layers correspond to BN chains (h-BN crystal layers), consisting from N_{bn} links. These layers are on a flat solid substrate and interact with it (let's assume, that solid substrate surface coincides with $z = 0$ plane). The last K-th G chain with $N_c \ll N_{bn}$ links corresponds to a carbon nanoparticle (nanoribbon, nanotube) on a flat deformed multilayer substrate. Coordinates of this system nodes with K chains are set with vectors $\{\mathbf{u}_{n,k} = (x_{n,k}, z_{n,k})\}_{n=1,k=1}^{N_k,\ K}$, where N_k — number of nodes in k-th chain ($N_k = N_{bn}$ at $k = 1, K-1$ and $N_K = N_c$).

Hamiltonian of the chain system will be the following

$$H = \sum_{k=1}^{K-1}\sum_{n=1}^{N_{bn}} \frac{1}{2} c M_2(\dot{\mathbf{u}}_{n,k}, \dot{\mathbf{u}}_{n,k}) + \sum_{n=1}^{N_c} \frac{1}{2} M_1(\dot{\mathbf{u}}_{n,K}, \dot{\mathbf{u}}_{n,K}) + E, \tag{7}$$

where potential energy

$$E = c\sum_{k=1}^{K-1}\left[\sum_{n=1}^{N_{bn}-1} V_2(R_{n,k}) + \sum_{n=2}^{N_{bn}-1} U_2(\theta_{n,k}) + \sum_{n=1}^{N_{bn}} W_0(z_{n,k})\right] \tag{8}$$

$$+ c\sum_{k_1=1}^{K-2}\sum_{k_2=k_1+1}^{K-1}\sum_{n=1}^{N_{bn}}\sum_{l=1}^{N_{bn}} W_1(r_{n,k_1;l,k_2}) \tag{9}$$

$$+ \sum_{n=1}^{N_c-1} V_1(R_{n,K}) + \sum_{n=2}^{N_c-1} U_1(\theta_{n,K}) \tag{10}$$

$$+ \sum_{k=1}^{K-1}\sum_{n=1}^{N_{bn}}\sum_{l=1}^{N_c} W_2(r_{n,k;l,K}). \tag{11}$$

Here a distance between adjacent nodes of k-th chain $R_{n,k} = |\mathbf{u}_{n+1,k} - \mathbf{u}_{n,k}|$, angle cosine between two adjacent bonds

$$\cos(\theta_{n,k}) = -(\mathbf{v}_{n-1,k}, \mathbf{v}_{n,k})/R_{n-1,k}R_{n,k},$$

vector $\mathbf{v}_{n,k} = \mathbf{u}_{n+1,k} - \mathbf{u}_{n,k}$, distance between the nodes of different chains k_1 and k_2 $r_{n,k_1;l,k_2} = |\mathbf{u}_{l,k_2} - \mathbf{u}_{n,k_1}|$. First term (8) of potential energy formula sets a deformation energy of BN chains considering energy of their interaction with a solid substrate, the second term (9) — energy of non-valence interaction of BN chains, the third term (10) — energy of deformation of G chain, and the last term (11) — energy of non-valence interaction of G chain with BN chains.

Table 1. Values of parameters of Lennard–Jones potential (4) for various pairs of interacting atoms [30].

	BB	NN	BN	CB	CN
ϵ_0 (meV)	7.81	2.99	4.81	5.96	3.69
r_0 (Å)	4.083	3.660	3.866	3.976	3.756

3. Nanoparticles motion on thermalized substrate

Let's examine a system, consisting of $K-1=3$ layers of BN chains with $N_{bn}=2400$ links. Length of such three-layer substrate $L=(N_{bn}-1)R_2=300.4\,\text{nm}$. Let's take linear (cyclical) G chain of N_c links as a carbon nanoparticle, located on this substrate.

At first, let's put the nanoparticle near the left edge of the substrate, as shown in Fig. 2. Then let's find the stationary state of a system „*nanoparticle + three-layer substrate*". For that let's numerically, using conjugate gradient method, solve this task for minimum of energy

$$E \to \min : \{\mathbf{u}_{n,k}\}_{n=1,k=1}^{N_k,\ K}, \tag{12}$$

where number of chains $K=4$, number of nodes $N_1=N_2=N_3=N_{bn}=2400$, $N_4=N_c$. Typical view of stationary states is shown in Fig. 2.

Let's put the system into Langevin thermostat for obtaining the thermalized state. For that we fixate x coordinates of the edge particles of BN chains (let's assume that speeds $\{\dot{x}_{1,k}\equiv 0,\ \dot{x}_{N_{bn},k}\equiv 0\}_{k=1}^{K-1}$) and x coordinate of the central particle of G chain ($\dot{x}_{N_c/2,K}\equiv 0$) and numerically integrate Langevin equation system

$$M_2\ddot{\mathbf{u}}_{n,k}=-\frac{1}{c}\frac{\partial H}{\partial \mathbf{u}_{n,k}}-\Gamma M_2\dot{\mathbf{u}}_{n,k}+\Xi_{n,k},$$

$$k=1,\ldots,K-1,\ \ n=1,\ldots,N_{bn}, \tag{13}$$

$$M_1\ddot{\mathbf{u}}_{n,K}=-\frac{\partial H}{\partial \mathbf{u}_{n,K}}-\Gamma M_1\dot{\mathbf{u}}_{n,K}+\Xi_{n,K},$$

$$n=1,\ldots,N_c, \tag{14}$$

where $\Gamma=1/t_r$ — friction coefficient (relaxation time $t_r=0.4$ ps), $\Xi_{n,k}=(\xi_{n,k,1},\xi_{n,k,2})$ — two-dimensional vector of normally distributed random forces, normalized with conditions

$$\langle \xi_{n,k,i}(t_1)\xi_{m,l,j}(t_2)\rangle = 2M\Gamma k_B T\delta_{nm}\delta_{kl}\delta_{ij}\delta(t_2-t_1)$$

(T — thermostat temperature, k_B — Boltzmann constant, mass $M=M_2/c$ at $k<K$ and $M=M_1$ at $k=K$).

Let's take initial conditions for Langevin motion equation system (13), (14), corresponding to the main stationary condition of the system $\{\mathbf{u}_{n,k}(0)=\mathbf{u}^0_{n,k},\ \ \dot{\mathbf{u}}_{n,k}(0)=\mathbf{0}\}_{n=1,k=1}^{N_k,\ K}$ and numerically integrate the system for a time $t_0=20t_r$. Over this time the chain system will come to complete equilibrium with the thermostat, and we will get its thermalized state $\{\mathbf{w}_{n,k}=\mathbf{u}_{n,k}(t_0),\ \mathbf{v}_{n,k}=\dot{\mathbf{u}}_{n,k}(t_0)\}_{n=1,k=1}^{N_k,\ K}$.

For modeling of nanoparticle free motion over thermalized multilayer substrate let's leave only x coordinates of the edge nodes of BN chains as fixated, remove interaction of the system with the thermostat, and impart an additional initial speed $v_0>0$, directed along x axis, to all nanoparticle atoms. Let's integrate numerically the system of motion equations

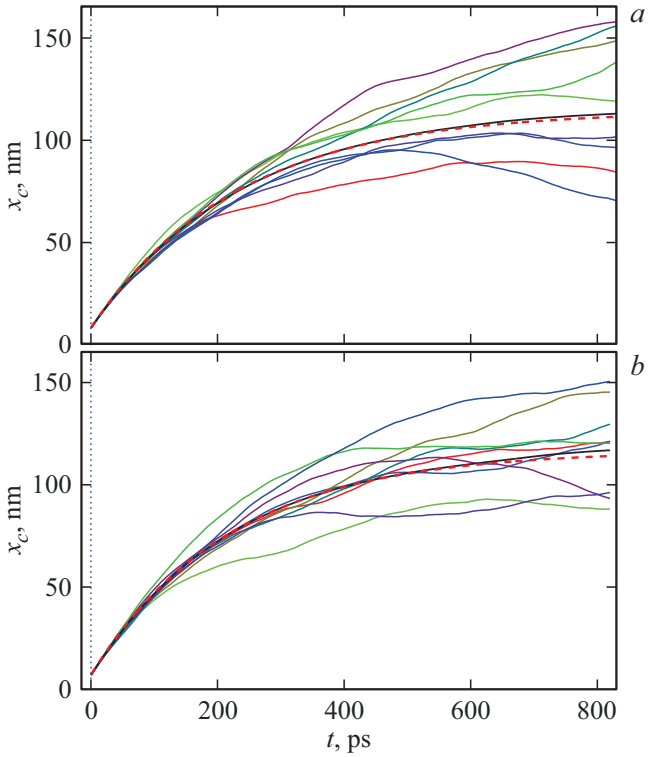

Figure 3. Dependence of gravity center of carbon nanoparticle x_c on time t at substrate temperature $T=300$K. Thin curves show 9 motion paths for various independent initial implementations of the system thermalized state. Solid heavy (black) line shows the path of the average value of the gravity center $\bar{x_c}$, obtained for 256 independent implementations of the thermalized state. Part (a) shows the dynamics for a linear chain (nanoribbon), part (b) — for a cyclical chain (nanotubes) with $N_c=40$ links, initial speed of nanoparticle motion $v_0=500$ m/s. Dashed (red) lines show dependence (19) at value of the effective friction coefficient $\gamma=4.32$ and $4.56\,\text{ns}^{-1}$.

$$M_2\ddot{\mathbf{u}}_{n,k}=-\frac{1}{c}\frac{\partial H}{\partial \mathbf{u}_{n,k}},$$

$$k=1,\ldots,K-1,\quad n=1,\ldots,N_{bn}, \tag{15}$$

$$M_1\ddot{\mathbf{u}}_{n,K}=-\frac{\partial H}{\partial \mathbf{u}_{n,K}},\quad n=1,\ldots,N_c, \tag{16}$$

with initial conditions

$$\mathbf{u}_{n,k}(0)=\mathbf{w}_{n,k},\ \ \dot{\mathbf{u}}_{n,k}(0)=\mathbf{v}_{n,k},$$

$$n=1,\ldots,N_{bn},\ \ k=1,\ldots,K-1, \tag{17}$$

$$\mathbf{u}_{n,K}(0)=\mathbf{w}_{n,K},\ \ \dot{\mathbf{u}}_{n,K}(0)=\mathbf{v}_{n,K}+v_0\mathbf{e}_x,$$

$$n=1,\ldots,N_c, \tag{18}$$

where vector $\mathbf{e}_x=(1,0)$.

Let's track the motion of nanoparticle gravity center $x_c=(x_{1,K}+x_{2,K}+\ldots+x_{N_c,K})/N_c$ along the substrate. Carbon nanoparticles (nanoribbons and nanotubes) motion

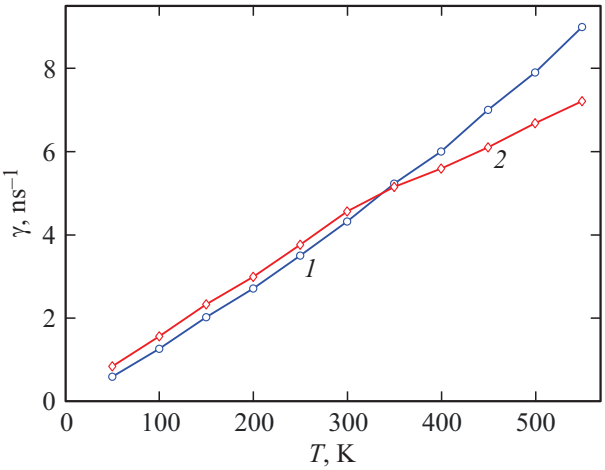

Figure 4. Dependence of friction coefficient γ on temperature T for linear (nanoribbons) and cyclical chain (nanotubes) of $N_c = 40$ links (curve *1* and *2*).

nature is shown in Fig. 3. As seen from the figure, form of path $x_c(t)$ depends on implementation of initial thermalized state of the system, but interaction with the substrate always results in deceleration of the particle directed motion (initial motion speed $v_0 = 500$ m/s). If we average the paths by all independent implementations of the system thermalized state (take the average value of $\bar{x_c}(t) = \langle x_c(t) \rangle$), the dynamics of the nanoparticle gravity center is described with good accuracy as particle motion in viscous medium

$$\bar{x_c}(t) = \bar{x_c}(0) + v_0[1 - \exp(-\gamma t)]/\gamma, \qquad (19)$$

with coefficient of viscous „friction" $\gamma > 0$ (inverse value γ^{-1} corresponds to time, over which the particle initial speed reduces by a factor of e). Thus, at $N_c = 40$ and temperature $T = 300$ K the coefficient of effective friction for motion over nanoribbon and nanotube substrate $\gamma = 4.32$ and $4.56\,\text{ns}^{-1}$ — see Fig. 3 (*a*) and (*b*).

Numerical modeling of nanoparticles dynamics showed, that its viscous deceleration (19) happens at all nanoparticles sizes and substrate temperatures $50 \le T \le 550$ K, but value of effective friction coefficient γ depends on temperature, size and type of nanoparticle. Dependence of γ on temperature is shown in Fig. 4. As seen from the figure, the friction coefficient monotonously grows with temperature increase. At $T \le 300$ K the temperature reduction results in almost linear reduction of effective friction γ to values, close to zero. It allows to conclude, that the reason for nanoparticles deceleration is their interaction with thermal vibrations. Bending (transverse) chains vibrations play the main role in this interaction — with their amplitude decrease the effective friction also significantly reduces.

It should be noted, that the obtained significant growth of friction with temperature increase paradoxically differs from standard friction scenarios, where it always reduces with temperature increase [31]. The difference is caused by the fact, that in the examined system the friction has a wave nature (caused by interaction with thermal vibrations). Increase of friction force of layers of G/h-BN with temperature increase was also observed in the work [32].

4. Thermophoresis force

For direct heat transfer modeling let's put the first $N_t = 40$ nodes of the substrate chain into the Langevin thermostat with temperature T_+, while the last ones — into thermostat with temperature T_- (temperature difference $\Delta T = T_+ - T_- \ge 0$). Then we need to numerically integrate the system of equations for heat transfer modeling along the substrate:

$$M_2 \ddot{\mathbf{u}}_{n,k} = -\frac{1}{c}\frac{\partial H}{\partial \mathbf{u}_{n,k}} - \Gamma M_2 \dot{\mathbf{u}}_{n,k} + \Xi^+_{n,k}, \quad n = 1, \ldots, N_t,$$

$$M_2 \ddot{\mathbf{u}}_{n,k} = -\frac{1}{c}\frac{\partial H}{\partial \mathbf{u}_{n,k}}, \quad n = N_t + 1, \ldots, N_{bn} - N_t, \qquad (20)$$

$$M_2 \ddot{\mathbf{u}}_{n,k} = -\frac{1}{c}\frac{\partial H}{\partial \mathbf{u}_{n,k}} - \Gamma M_2 \dot{\mathbf{u}}_{n,k} + \Xi^-_{n,k},$$

$$n = N_{bn} - N_t + 1, \ldots, N_{bn}, \ k = 1, \ldots, K-1,$$

$$M_1 \ddot{\mathbf{u}}_{n,K} = -\frac{\partial H}{\partial \mathbf{u}_{n,K}}, \quad n = 1, \ldots, N_c,$$

where $\Gamma = 1/t_r$ — friction coefficient (relaxation time $t_r = 0.4$ ps), $\Xi^{\pm}_{n,k} = (\xi^{\pm}_{n,k,1}, \xi^{\pm}_{n,k,2})$ — two-dimensional vector of normally distributed random forces, normalized with conditions

$$\langle \xi^{\pm}_{n,k,i}(t_1) \xi^{\pm}_{m,l,j}(t_2) \rangle = 2M_2 \Gamma k_B T_{\pm} \delta_{nm} \delta_{kl} \delta_{ij} \delta(t_2 - t_1).$$

Let's take initial conditions for the motion equation system (20), corresponding to the ground state of multilayer system with graphene chain location in the substrate center. Let's fixate x coordinate of the central particle of G chain (assume that $\dot{x}_{N_c/2,K} \equiv 0$) and numerically integrate the motion equation system until formation of stationary heat flow. In the central part of the substrate $N_t < n \le N_{bn} - N_t$ the constant temperature gradient forms — see Fig. 5. Distribution of the average temperature values along the substrate was obtained as per formulas:

$$\bar{T_n} = \langle T_n \rangle = \lim_{t \to \infty} \frac{M_2}{2(K-1)k_B t} \int_0^t \sum_{k=1}^{K-1} |\dot{\mathbf{u}}_{n,k}(\tau)|^2 d\tau.$$

Let's also find the average values of longitudinal forces $F_{n,1}$, acting from substrate side to the nodes of G chain. Full force vector

$$\mathbf{F}_n = (F_{n,1}, F_{n,2}) = \sum_{k=1}^{K-1} \sum_{l=1}^{N_{bn}} \frac{\partial W_2(r_{l,k;n,K})}{\partial \mathbf{u}_{n,K}},$$

where distance $r_{l,k;n,K} = |\mathbf{u}_{n,K} - \mathbf{u}_{l,k}|$.

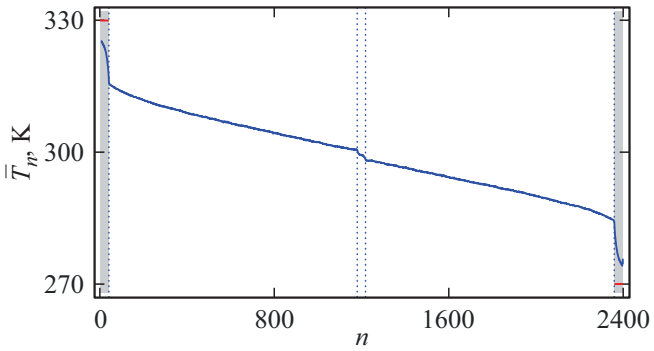

Figure 5. Distribution of local temperature $\bar{T}_n$ along three-layer substrate. Each substrate chain contains $N_{bn} = 2400$ links. Edge thermostats temperature $T_{\pm} = 300 \pm 30$ K, number of edge links, interacting with thermostats, $N_t = 40$. Edge substrate sections, interacting with thermostats, are shown with grey color. Temperature profile distortion in the substrate center is related to presence of G chain of $N_c = 40$ links.

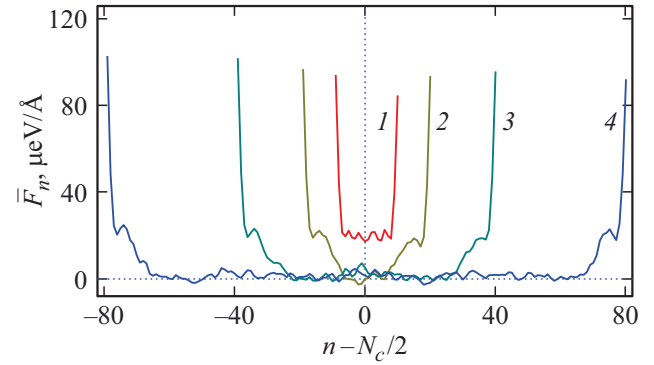

Figure 6. Distribution of thermophoresis forces $\bar{F}_n$ along G chain at number of the chain links $N_c = 20$, 40, 80, 160 (curves *1, 2, 3, 4*). Each substrate chain contains $N_{bn} = 2400$ links, edge thermostats temperature $T_{\pm} = 300 \pm 30$ K.

Let's assume that

$$\bar{F}_{n,1} = \lim_{t\to\infty} \frac{1}{t} \int_0^t F_{n,1}(\tau)d\tau$$

— the average value of longitudinal force, acting from substrate side to node n of G chain at heat flow presence, and $\bar{F}^0_{n,1}$ — the average value of force without heat flow (at $T_{\pm} = T$). Then the heat flow presence will result in formation of additional forces $\bar{F}_n = \bar{F}_{n,1} - \bar{F}^0_{n,1} > 0$, acting to G chain nodes in flow direction.

Distribution of thermophoresis forces $\bar{F}_n$ along G chain (along graphene nanoribbon) is shown in Fig. 6. As seen from the figure, the thermophoresis forces mainly acts on the nanoribbon edges, where bending substrate vibrations from phonons heat flow enter below graphene nanoribbon and exit from beneath it. It should be noted, that increase of the bending stiffness of substrate chains results in significant reduction of thermophoresis forces, thus indicating the main contribution of graphene nanoribbon interaction with the bending substrate vibrations to thermophoresis forces.

Table 2. Dependence of general F, edge F_e and central thermophoresis force F_c on number of links of G chain N_c (on graphene nanoribbon length) at substrate length $L = 300.4$ nm ($N_{bn} = 2400$) and temperature $T_{\pm} = 300 \pm 30$ K

N_c	20	40	80	160	320	640
F (10^{-6}eV/Å)	586	610	703	828	966	1186
F_e (10^{-6}eV/Å)	586	609	641	661	699	712
F_c (10^{-6}eV/Å)	0	1	62	166	267	356

Let's define the general $F = \sum_{n=1}^{N_c} \bar{F}_n$, central $F_c = \sum_{n=16}^{N_c-15} \bar{F}_n$ and edge thermophoresis force $F_e = F - F_c$.

Dependence of thermophoresis forces on graphene nanoribbon length (on number of nodes of G chain N_c) is presented in Table 2. As seen from the table, the general thermophoresis force monotonously increases with nanoribbon length increase. The main contribution to thermophoresis is made by the forces, acting on the 15 edge links of G chain, while the general force growth mainly happens due to increase of interaction with the central chain part of the substrate.

Heat transfer modeling showed, that thermophoresis force F is always directly proportional to temperature difference ΔT — see Fig. 7. From the other side, increase of distance between thermostats (substrate length increase) does not result in significant reduction of thermophoresis force. Thus, for G chain of $N_c = 40$ links at $T_{\pm} = 300 \pm 30$ K the thermophoresis force $F = 790$ at number of links in substrate chains $N_{bn} = 300$, $F = 830$ at $N_{bn} = 600$, $F = 770$ at $N_{bn} = 1200$ and $F = 610\,\mu$eV/Å at $N_{bn} = 2400$. This is related to the fact, that thermophoresis force is mainly provided by pressure of transverse (bending) long-wave phonons of substrate chains on graphene nanoribbon, and these phonons have a high free path

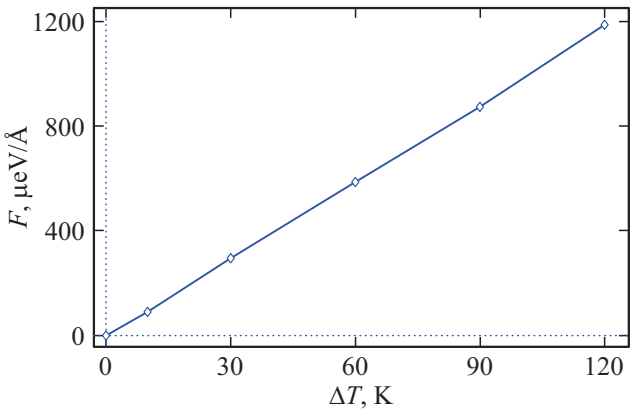

Figure 7. Dependence of thermophoresis force F on temperature difference of edge thermostats ΔT. Number of links of G chain $N_c = 20$, number of links in each substrate chain $N_{bn} = 2400$, average substrate temperature $T = 300$ K.

Table 3. Dependence of the established motion speed v_s of graphene nanoribbon (NR) and nanotube (NT) on number of chain links N_c at substrate length $L = 300.4$ nm ($N_{bn} = 2400$) and temperature $T_\pm = 300 \pm 30$ K

	N_c	20	40	80	160	320
NR	v_s (m/s)	289	291	283	279	276
NT	v_s (m/s)	296	284	283	290	286

length. Therefore, the effective nanoparticles transfer using thermophoresis can happen at significantly large distances.

5. Nanoparticles motion under heat flow action

The performed analysis allows to conclude, that nanoparticle motion on a flat multilayer substrate of h-BN can be described as its motion in viscous medium under constant force action

$$M\ddot{x}_c = F - \gamma M\dot{x}_c, \qquad (21)$$

where $M = N_c M_1$ — particle mass, x_c — x particle gravity center coordinate. From equation (21) it follows, that the particle will move in time with the established constant speed $v_s = F/\gamma M$.

Let's find the established nanoparticle motion speed v_s from direct numerical modeling of the particle dynamics over a substrate, over which the heat transfer happens. Let's integrate numerically the system of motion equations (20). At first, let's put the nanoparticle near the left substrate edge. Let's fixate x coordinate of node $N_c/2$ of G chain and integrate the system until formation of constant heat flow in the substrate. Then we impart the speed v_s to all G chain nodes and examine free motion of the chain over the substrate at thermal transfer presence.

Numerical modeling showed, that under heat flow action the nanoparticle on the substrate surface always reaches the mode of motion with constant speed $v_s > 0$ — see Fig. 8. Of course, the form of the motion path of the nanoparticle gravity center $x_c(t)$ depends on certain implementation of the thermalized state of the substrate. But if we average by all independent implementations of the initial thermalized substrate state, the gravity center motion will happen with constant speed:

$$\bar{x}_c(t) = \langle x_c(t) \rangle = \bar{x}_c(0) + v_s t. \qquad (22)$$

Dependence of stationary motion speed v_s on nanoparticle type and number of its links N_c is presented in Table 3. As seen from the table, the motion speed is almost the same for all types of nanoparticles. This indicates, that relation $F/\gamma M$ always remains almost the same for all carbon nanoparticles. This effect is caused by the fact, that thermophoresis force F and general friction coefficient γ have the same source — nanoparticle interaction with transverse thermal vibrations of the substrate layers.

Linear dependence of value of thermophoresis force F on temperature difference ΔT (Fig. 7) provides also linear dependence of stationary motion speed. Motion speed v_s

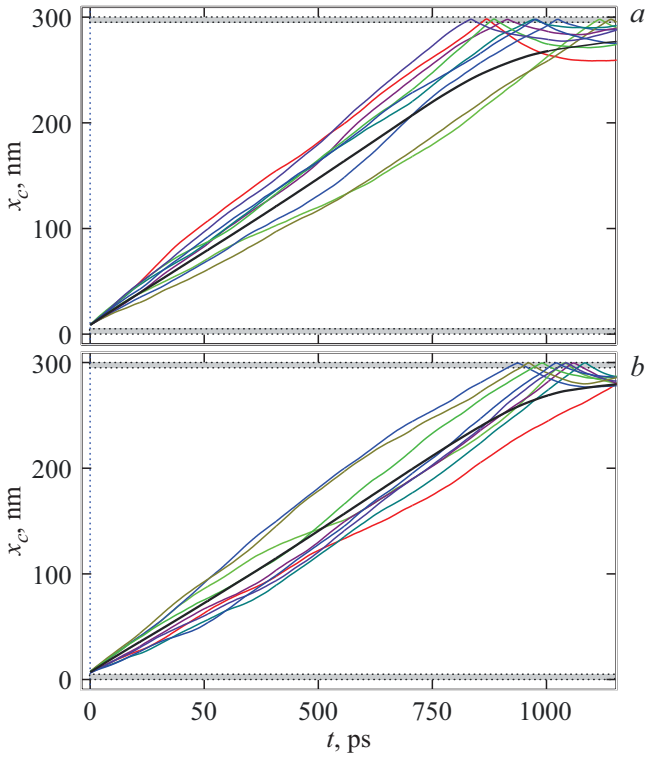

Figure 8. Dependence on time t of carbon nanoparticle gravity center x_c at temperature of edge thermostats $T_\pm = 300 \pm 30$ K (substrate edges, interacting with thermostats, are shown with grey color). Thin curves show 9 motion paths for various independent initial implementations of the substrate thermalized state. Solid heavy (black) line shows the path of the average value of the gravity center $\bar{x}_c$, obtained for 256 independent implementations of the thermalized state. Part (a) shows the dynamics for a linear chain (nanoribbon), part (b) — for a cyclical chain (nanotubes) with $N_c = 40$ links.

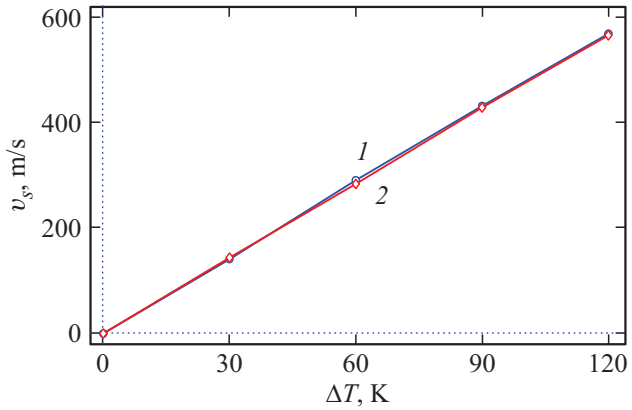

Figure 9. Dependence of the established nanoribbon and nanotube motion speed v_s (curve *1* and *2*) on temperature difference ΔT (edge thermostats temperature $T_\pm = T \pm \Delta T/2$, $T = 300$ K). Number of links of G chain $N_c = 40$, number of links of substrate chains $N_{bn} = 2400$.

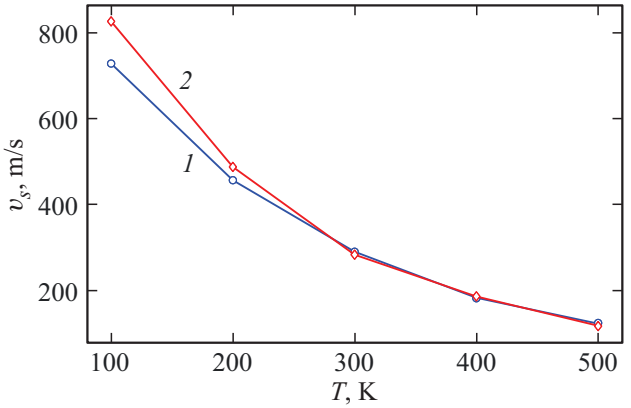

Figure 10. Dependence of the established nanoribbon and nanotube motion speed v_s (curve *1* and *2*) on average substrate temperature T. Number of links of G chain $N_c = 40$, number of links of substrate chains $N_{bn} = 2400$. Temperature of edge thermostats $T_{\pm} = T \pm 30\,\mathrm{K}$.

is always directly proportional to temperature difference — see Fig. 9.

Monotonous reduction of the general friction coefficient γ at reduction of substrate temperature T (Fig. 4) results, at constant temperature difference ΔT maintaining, in monotonous growth of the stationary nanoparticle motion speed v_s — see Fig. 10. Therefore, the effect of carbon nanoparticles thermophoresis over flat multilayer substrate of h-BN will be manifested the most in the low-temperature region.

6. Conclusion

The performed numerical modeling shows, that the carbon nanoparticles (nanoribbons and nanotubes) thermophoresis on flat multilayer substrate of h-BN has a high efficiency. Under action of temperature difference at the substrate edges ΔT the constant heat flow forms in it, resulting in directed nanoparticles motion from a warm substrate edge to a cold one.

Nanoparticles motion on the thermalized substrate is described with good accuracy as particles motion in viscous medium. Dynamics modeling showed, that viscous deceleration happens at all nanoparticles sizes and substrate temperatures. Value of coefficient of effective friction of a particle with a substrate γ monotonously increases with temperature increase. At $T \leq 300\,\mathrm{K}$ the temperature reduction results in linear reduction of γ to values, close to zero. The reason for nanoparticles deceleration is their interaction with substrate thermal vibrations. The bending (transverse) vibrations of substrate layers play the main role in this interaction.

Heat flow along the substrate results in formation of constant forces (thermophoresis forces), acting on nanoparticles nodes and which direction coincides with heat transfer direction. The calculations showed, the forces mainly acts on the graphene nanoribbons edges, where bending substrate vibrations from phonons heat flow enter and exit from beneath it. The general thermophoresis force F monotonously increases with nanoribbon length increase. The main contribution to it is made by the forces, acting on the 15 edge links, while the general force growth happens due to increase of interaction with the central chain (nanoribbon) part of the substrate.

Thermophoresis force F is always directly proportional to temperature difference ΔT. At the fixed value of ΔT the increase of distance between thermostats (substrate length increase) does not result in significant reduction of the force. This is related to the fact, that thermophoresis force is mainly provided by pressure of bending long-wave phonons of substrate layers on graphene nanoribbon, and these phonons have a high free path length. Therefore, the effective nanoparticles transfer using thermophoresis can happen at significantly large distances.

The nanoparticles motion under heat flow action on a flat multilayer substrate of h-BN can be described as their motion in viscous medium under action of the constant force F. Therefore, in time the particle will always move in heat flow direction with constant speed v_s. Dynamics modeling showed, that stationary motion speed is almost the same for all sizes and type of carbon nanoparticles. This effect is caused by the fact, that thermophoresis force F and general friction coefficient γ have the same source — nanoparticle interaction with transverse thermal vibrations of the substrate layers.

Value of speed v_s is always directly proportional to temperature difference. Monotonous reduction of the general friction coefficient γ at reduction of substrate temperature T at constant temperature difference ΔT maintaining results in monotonous growth of the nanoparticle motion speed. Therefore, the carbon nanoparticles thermophoresis on a flat multilayer substrate of h-BN will be manifested the most at low temperatures.

Funding

The study was carried out with the financial support of the Russian Foundation for Basic Research under the scientific project No. 18-29-19135. Computing resources are provided by the RAS Interdepartmental Center for Supercomputing.

Conflict of interest

The author declares that he has no conflict of interest.

References

[1] N. Azong-Wara, C. Asbach, B. Stahlmecke, H. Fissan, H. Kaminski, S. Plitzko, D. Bathen, T.A.J. Kuhlbusch. J. Nanopart. Res. **15**, 1530 (2013).

[2] A. Barreiro, R. Rurali, E.R. Hernandez, J. Moser, T. Pichler, L. Forro, A. Bachtold. Science **320**, 775–778 (2008).

[3] R. Piazza. Soft Matter **4**, *9*, 1740–1744 (2008).
[4] B. Liu, K. Zhou. Prog. Mater. Sci. **100**, 99–169 (2019).
[5] R. Guerra, U. Tartaglino, A. Vanossi, E. Tosatti Ballistic nanofriction. Nature Mater. **9**, 634–637 (2010).
[6] E. Panizon, R. Guerra, E. Tosatti. PNAS **114** (34), E7035 (2017).
[7] M. Jafary-Zadeh, C.D. Reddy, V. Sorkin, Y.-W. Zhang. Nanoscale Res. Lett. **7**, 148 (2012).
[8] A.V. Savin, Y.S. Kivshar. Transport of fullerene molecules along graphene nanoribbons. Sci. Rep. **2**, 1012 (2012).
[9] M. Becton, X. Wang. J. Chem. Theory Comput. **10**, 722 (2014).
[10] R. Rajegowda, S.K. Kannam, R. Hartkamp, S.P. Sathian. Nanotechbology **29**, *21*, 215401 (2018).
[11] D. Wang, L. Wang, Z. Hu. Nanoscale Res. Lett. **15**, 203 (2020).
[12] A. V. Savin, O.I. Savina. FTT, **63**, *4*, 564–571 (2021) (in Russian).
[13] P.A.E. Schoen, J.H. Walther, S. Arcidiacono, D. Poulikakos, P. Koumoutsakos. Nano Lett. **6**, *9*, 1910 (2006).
[14] P.A.E. Schoen, J.H. Walther, D. Poulikakos, P. Koumoutsakos. Appl. Phys. Lett. **90**, 253116 (2007).
[15] J. Shiomi, S. Maruyama. Nanotechnology **20**, 055708 (2009).
[16] E. Oyarzua, J.H. Walther, C.M Megaridis, P. Koumoutsakos, H.A. Zambrano. ACS Nano **11**, *10*, 9997 (2017).
[17] R. Rajegowda, S.K. Kannam, R. Hartkamp, S.P. Sathian. Nanotechnology **28**, 155401 (2017).
[18] E. Oyarzua, J.H. Walther, H.A. Zambrano. Phys. Chem. Chem. Phys. **20**, *5*, 3672 (2018).
[19] Q. Cao. J. Phys. Chem. C **123**, 29750 (2019).
[20] A. Panahi, P. Sadeghi, A. Akhlaghi, M.H. Sabour. Diamond & Related Materials **110** 108105 (2020).
[21] H.A. Zambrano, J.H. Walther, R.L. Jaffe. J. Chem. Phys. **131**, 241104 (2009).
[22] M.V.D. Prasad, B. Bhattacharya. Nano Lett., **16**, *4*, 2174 (2016).
[23] M.V.D. Prasad, B. Bhattacharya. Nano Lett. **17**, *4*, 2131 (2017).
[24] R. Rurali, E.R. Hernández. Chem. Phys. Lett. **497**, 62 (2010).
[25] N. Wei, H.-Q. Wang, J.-C. Zheng. Nanoscale Res. Lett. **7**, *1*, 154 (2012).
[26] A.V. Savin, E.A. Korznikova, S.V. Dmitriev, Phys. Rev. B **92**, 035412 (2015).
[27] A.V. Savin, E.A. Korznikova, S.V. Dmitriev, FTT **57**, *11*, 2278 (2015) (in Russian).
[28] A.V. Savin, E.A. Korznikova, S.V. Dmitriev, Phys. Rev. B **99**, 235411 (2019).
[29] J.H. Los, J.M.H. Kroes, K. Albe, R.M. Gordillo, M.I. Katsnelson, A. Fasolino. Phys. Rev. B **96**, 184108 (2017).
[30] A.K. Rappé, C.J. Casewit, K.S. Colwell, W.A. Goddard III, W.M. Skiff. J. Am. Chem. Soc. **114**, 10024 (1992).
[31] A. Vanossi, N. Manini, M. Urbakh, S. Zapperi, E. Tosatti, Rev. Mod. Phys. **85**, 529 (2013).
[32] D. Mandelli, W. Ouyang, O. Hod, M. Urbakh, Phys. Rev. Lett. **122**, 076102 (2019).